

AD-A116 055

NAVAL RESEARCH LAB WASHINGTON DC
PINCH-REFLEX-DIODE SCALING ON THE AURORA PULSER.(U)
JUN 82 R A MEGER, F C YOUNG
NRL-NR-4838

F/G 9/1

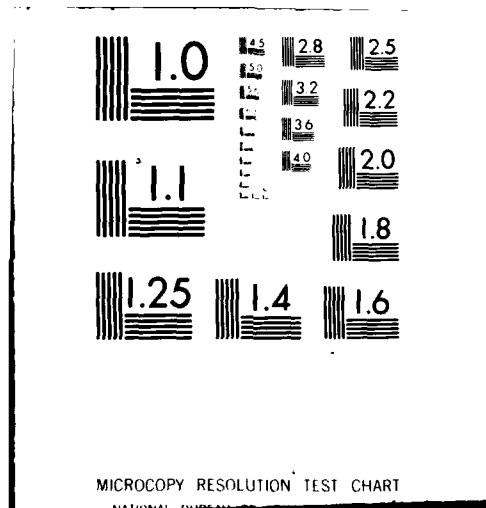
UNCLASSIFIED

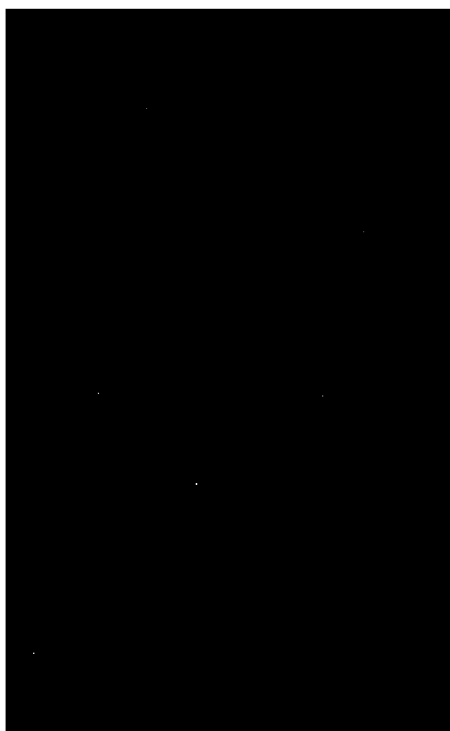
NL

100
and
1000



END
DATE
FILMED
7-82
DTIC





SECURITY CLASSIFICATION OF THIS PAGE (When Data Entered)

REPORT DOCUMENTATION PAGE		READ INSTRUCTIONS BEFORE COMPLETING FORM
1. REPORT NUMBER NRL Memorandum Report 4838	2. GOVT ACCESSION NO. AD-A116 055	3. RECIPIENT'S CATALOG NUMBER
4. TITLE (and Subtitle) PINCH-REFLEX-DIODE SCALING ON THE AURORA PULSER		5. TYPE OF REPORT & PERIOD COVERED Interim report on a continuing NRL problem.
7. AUTHOR(s) R. A. Meger* and F. C. Young		6. PERFORMING ORG. REPORT NUMBER
9. PERFORMING ORGANIZATION NAME AND ADDRESS Naval Research Laboratory Washington, DC 20375		8. CONTRACT OR GRANT NUMBER(s)
11. CONTROLLING OFFICE NAME AND ADDRESS Defense Nuclear Agency Washington, DC 20305		10. PROGRAM ELEMENT, PROJECT, TASK AREA & WORK UNIT NUMBERS T99QAXLA01; 47-0875-02
13. MONITORING AGENCY NAME & ADDRESS (if different from Controlling Office)		12. REPORT DATE 29
		13. NUMBER OF PAGES June 29, 1982
		15. SECURITY CLASS. (of this report) UNCLASSIFIED
		15a. DECLASSIFICATION/DOWNGRADING SCHEDULE
16. DISTRIBUTION STATEMENT (of this Report) Approved for public release; distribution unlimited.		
17. DISTRIBUTION STATEMENT (of the abstract entered in Block 20, if different from Report)		
18. SUPPLEMENTARY NOTES *Present address: JAYCOR, Inc., Alexandria, VA 22304. This research was sponsored by the Defense Nuclear Agency under Subtask T99QAXLA01, work unit 09 and work unit title "Ion Diode Research on Aurora Accelerator Product Area."		
19. KEY WORDS (Continue on reverse side if necessary and identify by block number) Pulsed power generator Plasma erosion switches Intense light ion beams Pinch reflex diode Neutron time of flight		
20. ABSTRACT (Continue on reverse side if necessary and identify by block number) A pinch-reflex ion diode has been operated on the Aurora pulser in positive polarity at impedances ranging from 10 to 35 Ω . Ion-generation efficiencies of 20% were observed with ion energies ranging from 2.5 to 5 MeV. The ion current scaled inversely with the anode-cathode gap, and a peak value of 65 kA was measured for the smallest gap. A plasma erosion switch was used to decrease prepulse and gap closure in the diode.		

DD FORM 1473
1 JAN 73

EDITION OF 1 NOV 68 IS OBSOLETE
S/N 0102-014-6601

SECURITY CLASSIFICATION OF THIS PAGE (When Data Entered)

/ii

CONTENTS

I. INTRODUCTION	1
II. ION-GENERATION-EFFICIENCY SCALING	2
III. EXPERIMENTAL PROCEDURE	3
IV. RESULTS	10
V. SUMMARY	21
ACKNOWLEDGMENTS	24
REFERENCES	24

DTIC
ELECTE
S JUN 25 1982 **D**
B



Accession For	
NTIS GRA&I	<input checked="" type="checkbox"/>
DTIC TAB	<input type="checkbox"/>
Unannounced	<input type="checkbox"/>
Justification	
By	
Distribution/	
Availability Codes	
Dist	Avail and/or Special
A	

PINCH-REFLEX-DIODE SCALING ON THE AURORA PULSER

I. Introduction

Progress in the field of intense pulsed light ion beam generation has been rapid over the last few years and high power ion beams are being investigated at several laboratories.¹ The Naval Research Laboratory (NRL) has concentrated its efforts on the pinch-reflex type of ion diode.² Experiments with this diode have been performed on the Gamble I and Gamble II accelerators at NRL,³ the PITHON accelerator at Physics International,⁴ and the Aurora accelerator at the Harry Diamond Laboratories.⁵ With these machines a large range of diode impedances and ion energies have been investigated. Ion beams have been produced with diodes operating at impedances of 1 to 35 Ω . Ion-generation efficiencies (ion current/diode current) of up to 60% have been achieved at the lower-impedance level. For higher-impedance diodes, efficiencies of up to 20% at 20 Ω and 5 MW have been measured. The dependence of the ion-beam output on various pinch-reflex-diode parameters is being studied in order to understand the scaling of such diodes with impedance and voltage.

The Aurora pulser is normally operated at high impedance (35 Ω) in negative polarity for bremsstrahlung production.⁶ Ion-diode experiments in negative polarity on this machine have been reported.⁵ Since then the accelerator has been modified to operate in positive-polarity. In this paper experiments on Aurora in positive polarity using a pinch-reflex-diode geometry are reported with emphasis on scaling of the ion-generation efficiency in the 10 to 35 Ω impedance regime. First, a simple scaling relationship for the ion efficiency of pinch-reflex diodes is presented. Then the experimental measurements and results are described. In particular, it is shown that the diode

efficiency is 20% at 10 Ω and 2.5 MV. Finally, the experimental results are compared with the expected scaling of the ion-beam-generation efficiency.

II. Ion-Generation-Efficiency Scaling

If a steady-state voltage is placed across a diode where electrons and ions are freely emitted from the cathode and anode surfaces, an equilibrium charge flow is established. This so called Child-Langmuir bipolar current scales as $V^{3/2}/D^2$ at nonrelativistic electron voltages where V is the diode voltage and D is the diode gap. The current is made up of electrons and ions streaming in opposite directions. In a planar diode most of the current is due to electron flow while the fraction of the current carried by ions depends on the electron to ion mass ratio. In the non-relativistic limit the relative current densities are given by

$$\frac{J_i}{J_e} = \left(\frac{M_e}{M_i}\right)^{1/2} \quad (1)$$

where J_i and J_e are the ion and electron current densities and M_e and M_i are the electron and ion masses. This calculation has been extended by Poukey to bipolar flow with relativistic electrons.⁷ It shows that the relative ion flux density should increase with diode voltage according to

$$\frac{J_i}{J_e} = \left(\frac{M_e}{2M_i}\right)^{1/2} (\gamma + 1)^{1/2}, \quad (2)$$

where γ is the relativistic factor for electrons at the full diode

voltage. Physically the γ dependence is due to electron-velocity saturation at relativistic energies. This means that for a bipolar diode ~2.3% of the diode current would be in protons for non-relativistic voltages versus 5.4% for the same planar diode operating at 5 MV when the electrons are relativistic.

Even with the current enhancement due to relativistic voltages as shown in Eq. 2, such ion-beam generators are relatively inefficient. One method of increasing the ion-generation efficiency beyond this level is to use a pinch-reflex-diode geometry as discussed by Goldstein and Lee.⁸ Such a diode geometry is shown schematically in Fig. 1. A cylindrical hollow cathode and thin planar anode foil force electrons to travel a longer distance than ions to cross the diode gap. Electrons emitted from the cathode are bent toward the axis by their self magnetic fields and may reflex through the anode foil on their way to the center stalk. For such a diode the relative ion current density to first order is given by

$$\frac{J_i}{J_e} = \left(\frac{M_e}{2M_i}\right)^{1/2} (\gamma + 1)^{1/2} \frac{R}{D} \quad (3)$$

where R is the cathode radius and D is the diode gap. For large R/D the pinch-reflex geometry can yield an order of magnitude increase in ion efficiency. Diodes with ion efficiency approaching 50% provide useful sources for intense ion beams.

III. Experimental Procedure

These experiments were performed on the Aurora accelerator operated in positive polarity to allow direct diagnostic access to the ion

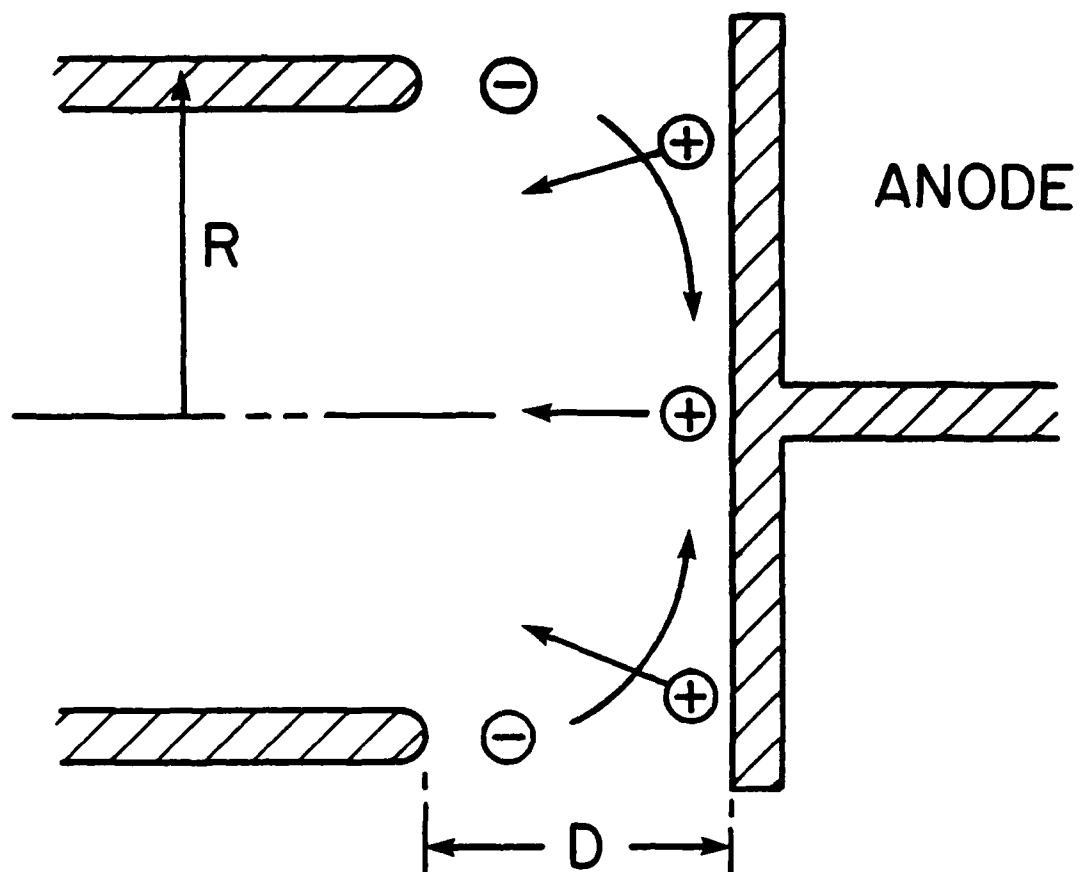


Fig. 1 — Pinch-reflex-diode schematic with conceptual electron and ion trajectories

beam. The Marx generator was charged to +90 kV out of a possible charge of +120 kV. The lower charge level was used to minimize possible damage to the Blumlein in positive polarity and to limit the voltage across the diode insulator. Only one of four vacuum transmission lines on the generator was used. Copper sulphate dummy loads were installed in the oil on the three unused lines.

The output end of the transmission line on the accelerator with the diode is shown in Fig. 2. The Blumlein output breaks down an oil prepulse switch putting the voltage pulse across the cylindrical insulator tube. This pulse propagates 7 meters along a magnetically insulated 50- Ω coaxial transmission line. The 1.2-m outer diam coaxial conductor is reduced to a 25-cm diam vacuum chamber at the front end while the 58-cm inner diam conductor is tapered to 10 cm. The ion diode is mounted one meter into this smaller diam coax. A flashover prepulse switch mounted on the inner conductor, as shown in Fig. 2, lowers the ~200-kV prepulse on the transmission line to less than 50 kV. On some shots a plasma erosion switch (PES) was used to further suppress the prepulse as well as to sharpen the risetime of the main pulse.

A cross sectional view of the PES system is shown in Fig. 3. The plasma guns for this system were supplied by Sandia National Laboratory⁹ and similar systems have been used elsewhere.¹⁰ Several microseconds before the main power pulse arrives, the plasma guns inject columns of carbon plasma with electron densities in the 10^{11} - 10^{12} cm^{-3} range into the coaxial vacuum transmission line. These columns short the inner and outer conductors by providing a low impedance shunt in parallel with the ion diode located downstream. This protects the ion-diode load from the machine prepulse as well as diverting some fraction of the main voltage

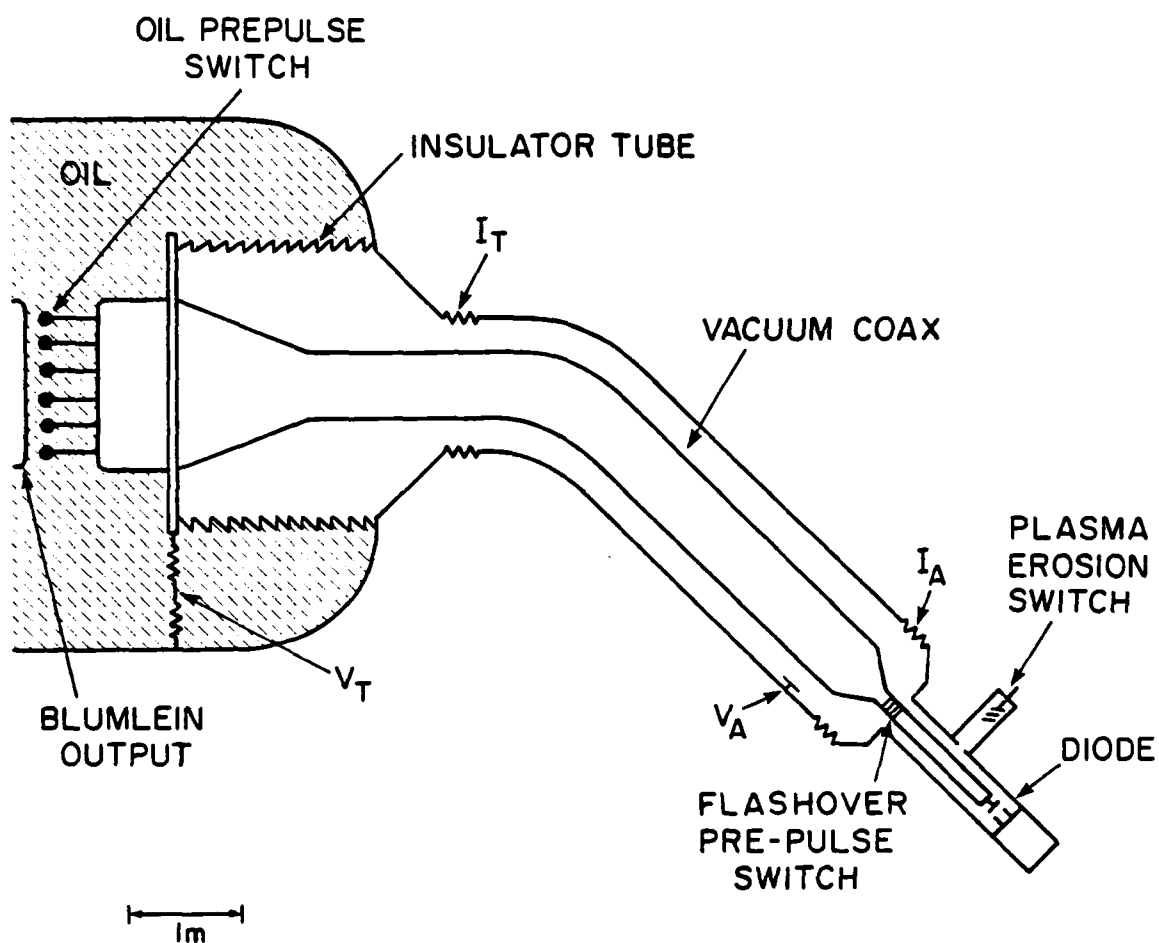


Fig. 2 — One arm of the Aurora pulser from the oil region to the ion diode. The location of the resistive voltage divider (V_T), the current shunt (I_A), the flashover prepulse switch and the plasma-erosion-switch system are shown.

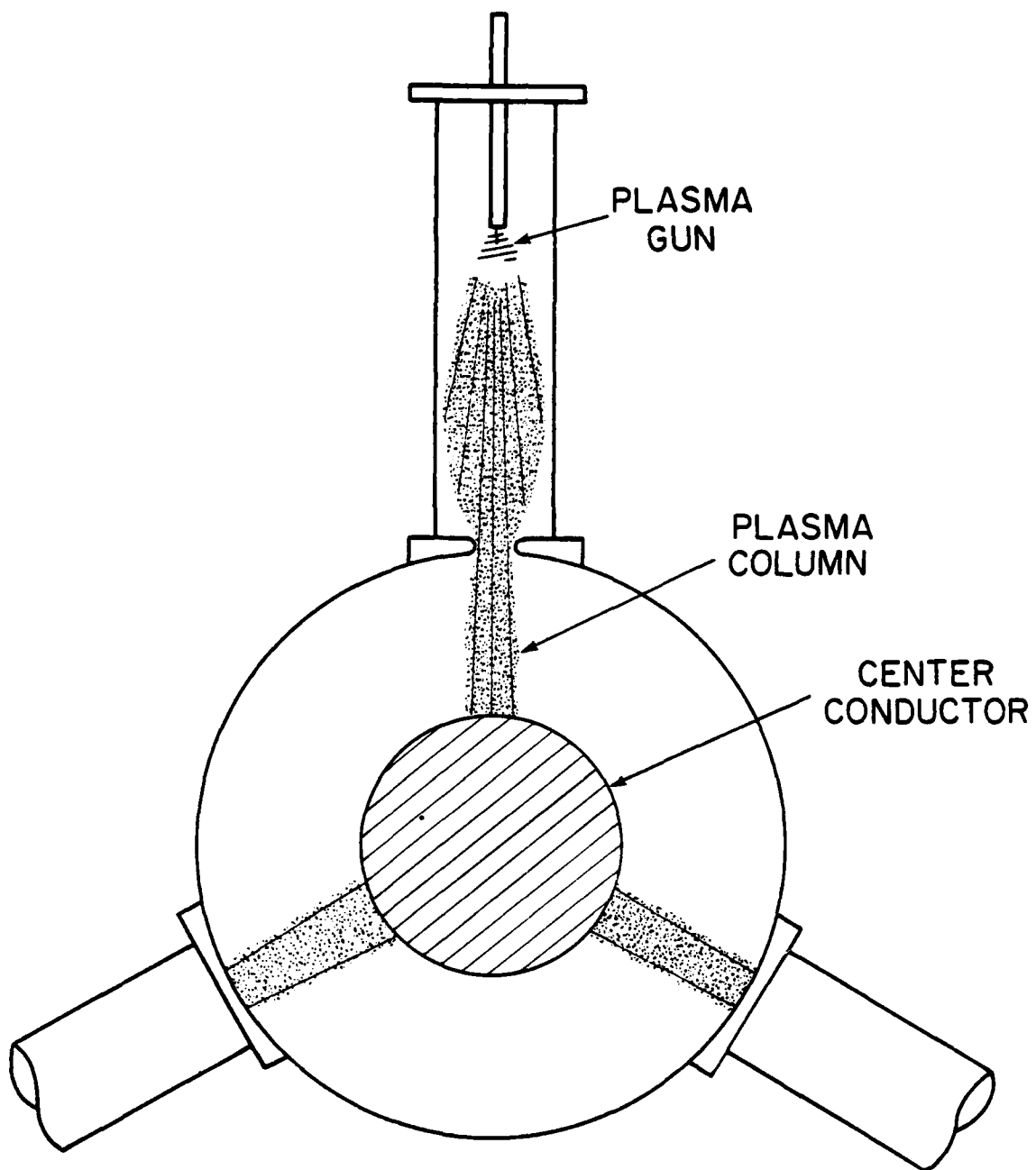


Fig. 3 — Cross-sectional schematic of the plasma-erosion-switch system

pulse. After the plasma columns have transmitted a certain amount of charge, the ion background density in the columns erodes near the outer injection aperture leading to sheath formation and a rapid decrease in the current diverted through the columns. The columns act as an opening switch, after which the remainder of the power pulse is delivered to the diode load. The prepulse and the leading edge of the main pulse have been shunted, and the voltage risetime across the load becomes the PES opening time which under most circumstances is less than the normal accelerator voltage risetime. The fraction of the main voltage pulse which is diverted through the erosion switch can be controlled by adjusting the injected plasma density. This is done by altering the distance of the plasma guns from the center conductor and the firing time of the guns.

The ion diode used in these experiments is shown in Fig. 4. The anode consists of a 127- μm thick polyethylene (CH_2) foil stretched on a 12-cm diam aluminum ring and supported by a thin-wall (0.17 mm) aluminum tube. The cathode is a 10-cm inner diam, 6.4-mm thick aluminum cylinder with a rounded end. On some shots a 2- μm thick aluminized foil (Kimfol*) is located inside the cathode followed by an aluminum witness plate coated with LiCl for neutron diagnostics. A Rogowski coil is mounted behind the cathode to measure the ion current incident on the Kimfol. This probe remains at ground potential with the generator configured in positive polarity.

The locations of the accelerator electrical diagnostics are shown in Fig. 2. The resistive voltage divider V_T , located in oil near the insulating tube, provides the most reliable voltage monitor. Capacitive

*Available from Kimberly Clark Corp., Lee, Mass. 01238

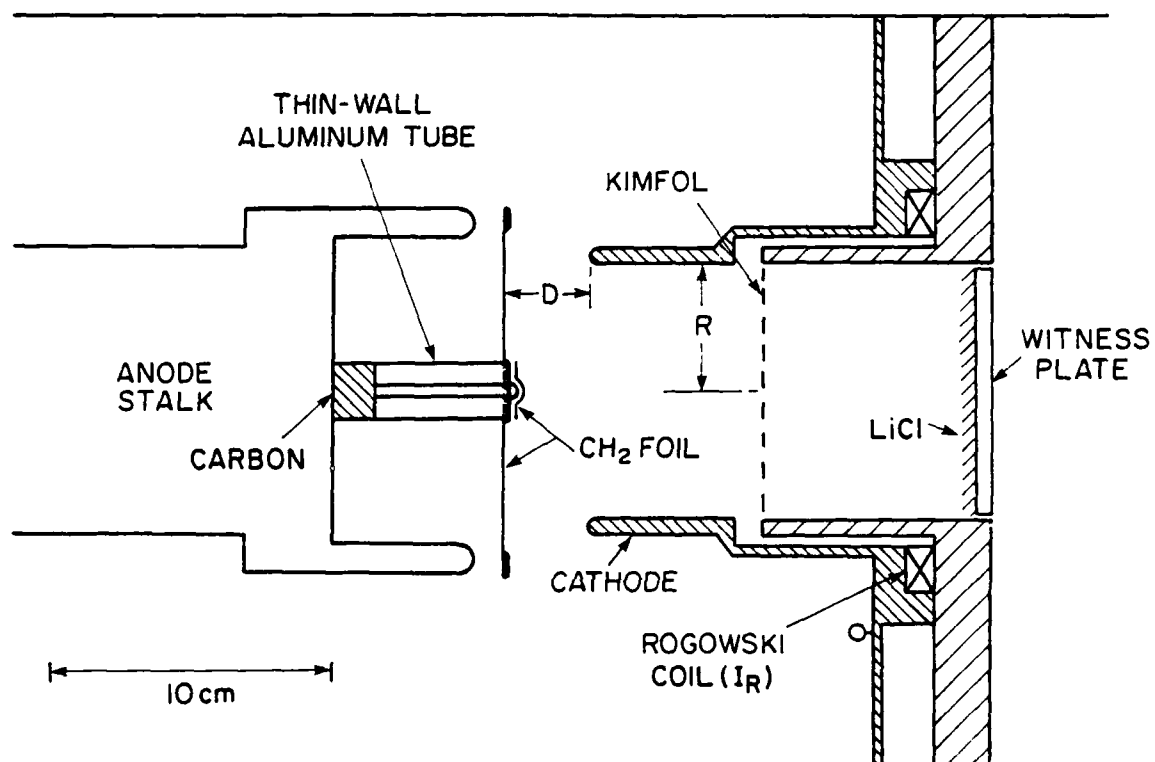


Fig. 4 — Details of the ion diode used in positive polarity

voltage probes located in the vicinity of V_A in the magnetically-insulated transmission line suffer from electron emission or collection and do not provide useable data. Resistive current shunts located on the outer conductor provide reliable signals but do not measure current due to electrons flowing in the vacuum along the surface of the outer conductor. The magnitude of such electron current is expected to be small at the relatively low electric fields present in the large diam coax region.

The electron and ion-beam diagnostics used in the experiment are shown in Fig. 5. These are similar to the previous negative-polarity experiments.⁵ Time integrated x-ray emission from the diode was imaged with a pinhole camera, while a scintillator-photodiode measured the time resolved x-ray signal. The ion diagnostics are based primarily on measurements of neutrons from the ${}^7\text{Li}(p,n){}^7\text{Be}$ reaction resulting from proton bombardment of the LiCl target. Neutron intensities were measured with a Rh-activation detector¹¹ and with Mn-activation detectors.¹² Neutron energies were measured with the time-of-flight (TOF) technique for flight paths of 10 to 15.2 meters in the forward direction. These energy measurements were used to determine the ion voltage for the diode.

IV. Results

Approximately 50 shots have been taken with anode-cathode (AK) gaps ranging from 1.5 to 5.5 cm with and without the plasma erosion switches. Pinching of the electron-beam on the anode axis as in negative-polarity experiments⁵ was confirmed by x-ray images from the pinhole camera. For a 2.0-cm AK gap, the diode operated at 2.5 MeV and

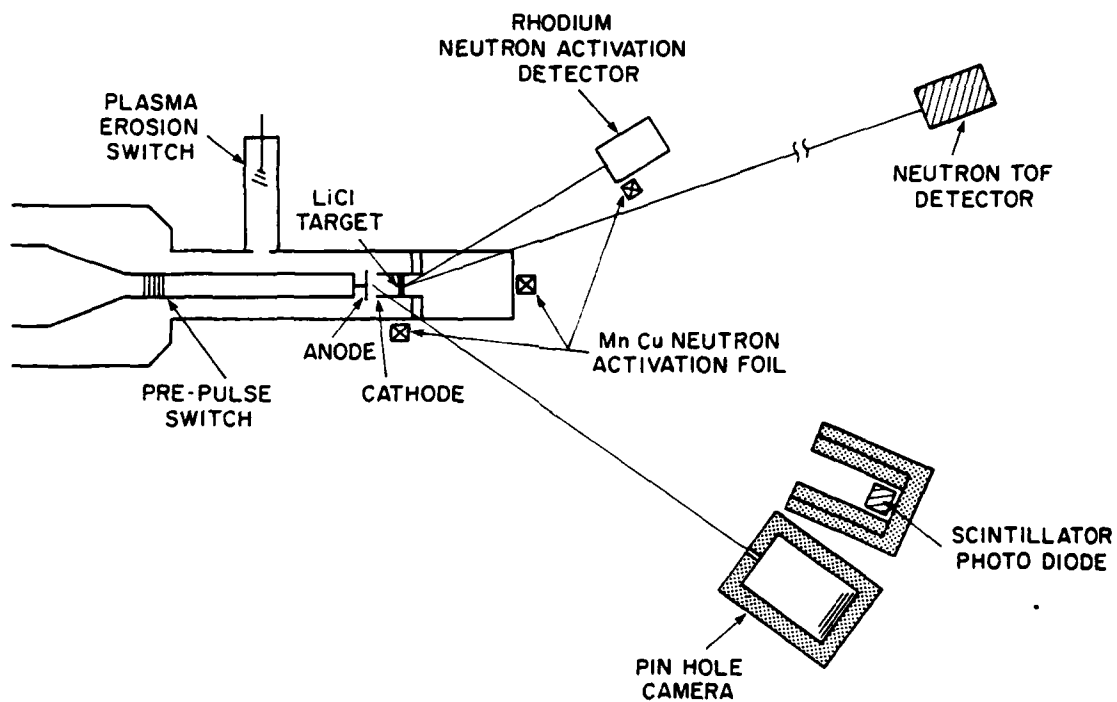


Fig. 5 — Schematic arrangement of the x-ray and neutron diagnostics

10 Ω (inferred from neutron TOF and total current measurements), while for a 5-cm AK gap the diode operated at 5 MeV and 35 Ω .

The large variation of the diode load impedance modified the power flow in the accelerator significantly. At low impedance the mismatch between the diode and the accelerator limited the amount of power delivered to the load. In addition the voltage measured across the insulator tube was found to be dependent on the load impedance. Figure 6 shows the behavior of the tube voltage for two shots with AK gaps of 5.5 cm and 3.0 cm. The large-AK-gap shot (No. 3057) ran at a higher tube voltage and impedance than the smaller-AK-gap shot (No. 3509). In general shots with lower peak tube voltage had longer-duration voltage pulses. This trade off between high voltage and pulse duration is demonstrated in Fig. 7 where the peak tube voltage (V_T) is plotted against the full-width-at-half-maximum (FWHM) of the voltage pulse for many shots with different AK gaps. This behavior of the tube voltage may be a consequence of the insulator design. The insulator was built for negative-polarity operation and can withstand 150-ns FWHM, 12-MV peak voltage pulses normally used in the bremsstrahlung mode. Using the same insulator for positive polarity degrades its voltage standoff by about a factor of two.¹³ The insulator flashover process is time and voltage dependent with higher voltages giving faster breakdown as indicated by the experimental data in Fig. 7. An attempt to suppress insulator flashover was made by placing a 120- Ω copper sulphate resistor across the insulator stack in parallel with the diode load. Shots with this resistor in place are indicated by open circles in Fig. 7. The resistor did cause the pulse duration to increase, but the dependence of the peak tube voltage on the duration of the tube voltage is still

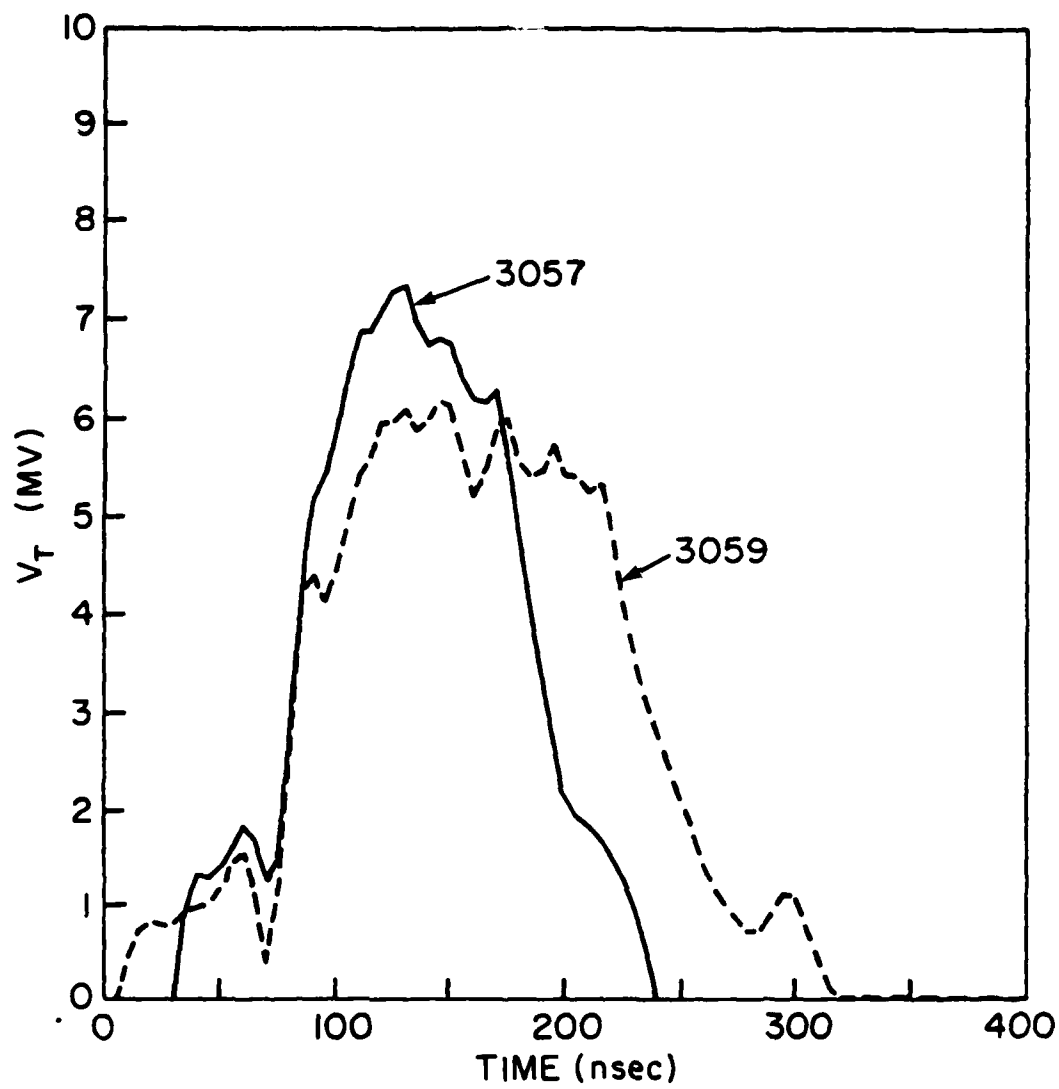


Fig. 6 — Measured tube voltages (V_T) for a 5.5-cm-AK-gap shot (No. 3057) and for a 3.0-cm-AK-gap shot (No. 3059)

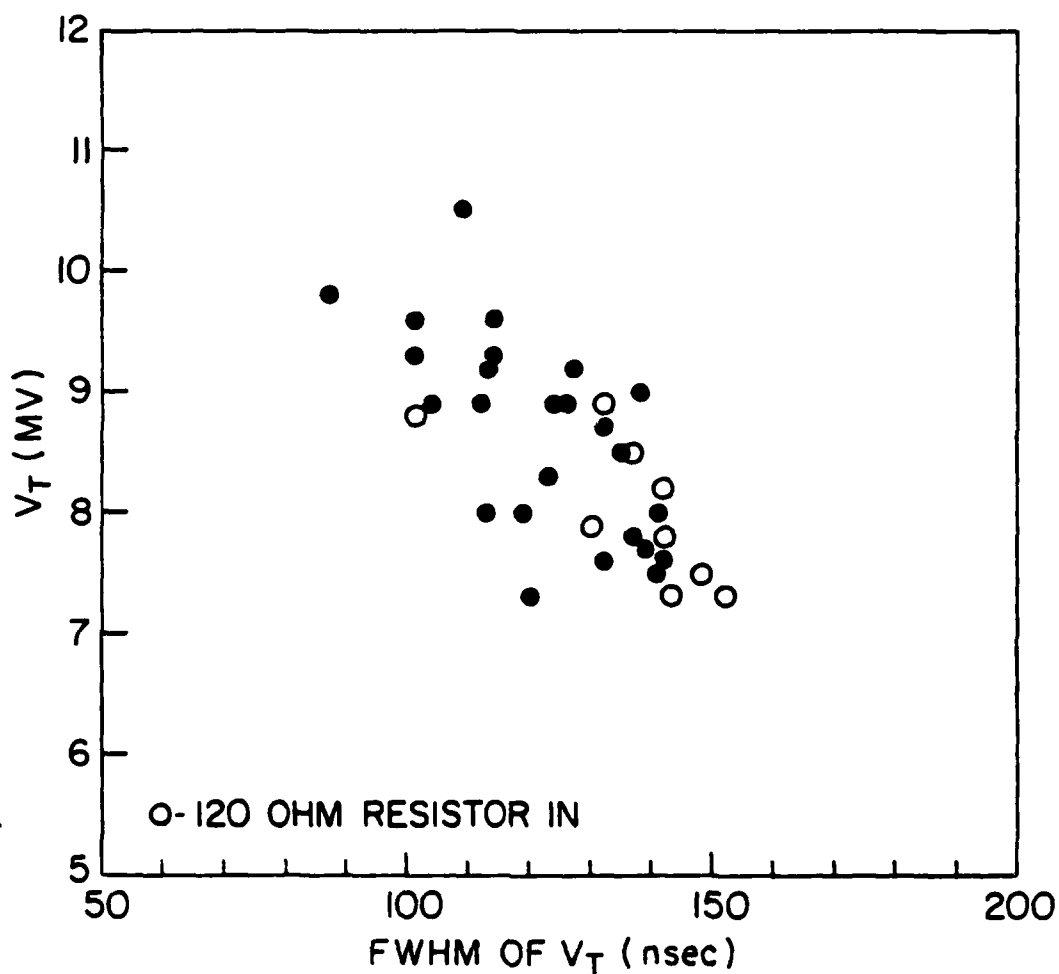


Fig. 7 — Dependence of the peak value of the tube voltage (V_T) on the full-width-at-half-maximum (FWHM) of the tube voltage. Shots with a 120- Ω resistor in parallel with the insulator are plotted as open circles.

evident. Thus for low impedance diodes the accelerator coupling limited power flow while at higher impedance the insulator flashover limited power flow. In all cases the peak power was less than 1 TW.

The dependences of the peak shunt current, I_A , (see Fig. 2) and peak Rogowski-coil current, I_R , (see Fig. 3) on the AK gap are displayed in Figs. 8 and 9 respectively. In both cases, an inverse relationship between current and AK gap is observed. The shunt current measures the total diode current except for vacuum electron flow past the shunt. This electron flow is expected to be small in the large diameter vacuum coax region where the shunt resistor is located. The Rogowski coil measures the net ion current passing through the coil and does not record current lost in front of the coil or current shielded by co-moving electrons. Witness plate and surface damage in the diode indicate that ions striking the cathode before the Rogowski coil represent < 10% of the total ion current. Computer simulations¹⁴ of the behavior of electrons and ions in the diode suggest that co-moving electrons could shield as much as 20% of the total ion current.

The PES system was operated on about half of the shots in this experiment. The amount of plasma in the erosion-switch gap differed from shot to shot depending on the plasma-gun timing. The erosion-switch operation did not affect the inverse dependence of the shunt current on the AK gap (see Fig. 8). On some shots the plasma density was increased so that most of the pulse was shunted through the PES system. On these shots the peak shunt-current signal approached 300 kA independent of the AK gap.

The maximum Rogowski current of 65 kA peak value was measured at the smallest AK gap of 2 cm (see Fig. 9). Operation of the PES system

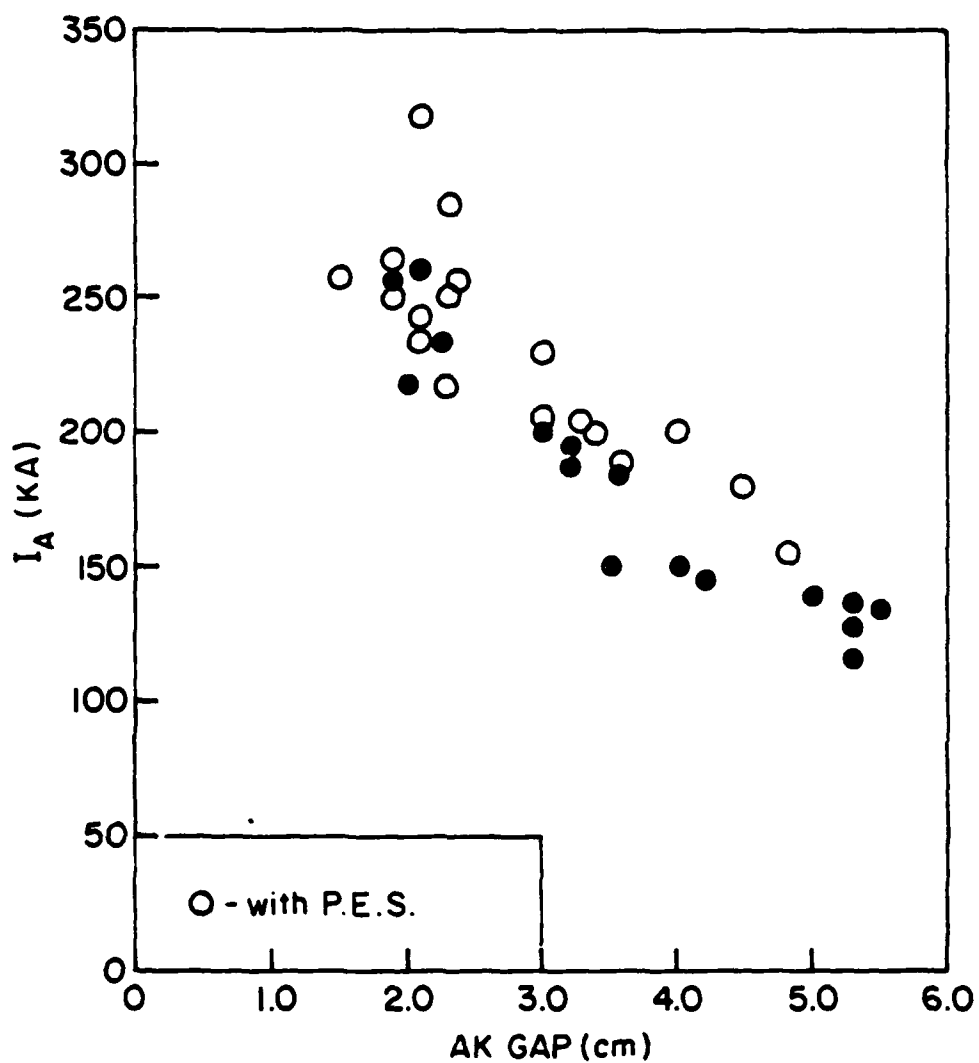


Fig. 8 — Dependence of the peak value of the shunt current (I_A) on the AK gap. Shots with the PES system operating are plotted as open circles.

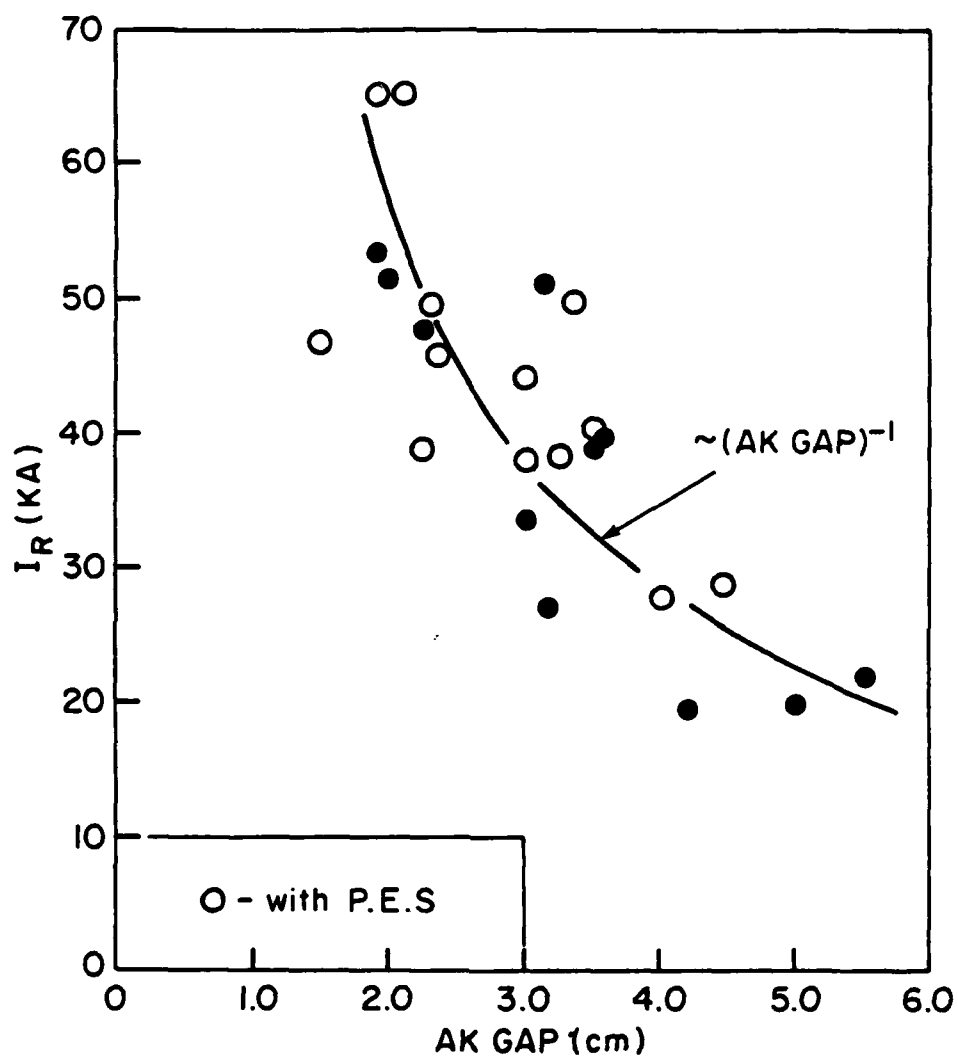
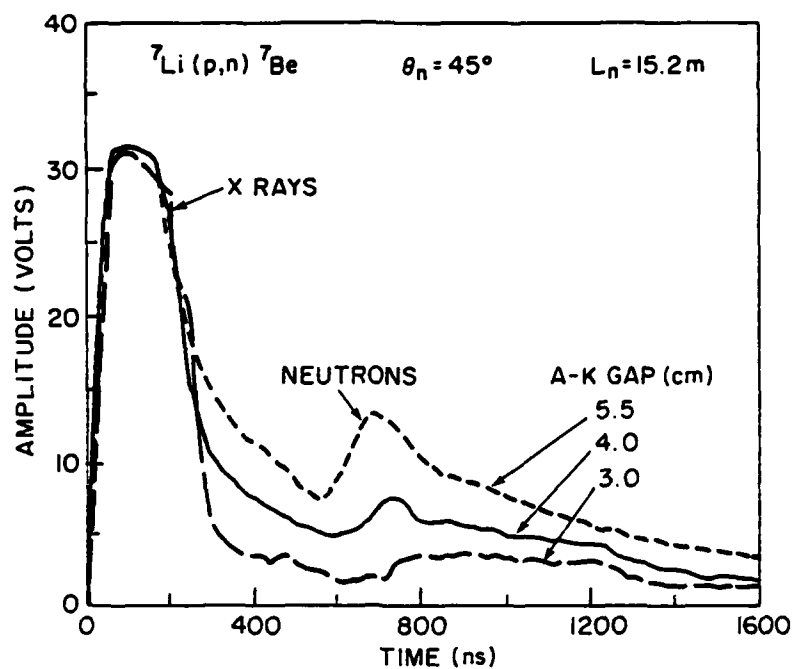


Fig. 9 — Dependence of the peak value of the Rogowski-coil current (I_R) on the AK gap. Shots with the PES system operating are plotted as open circles. The solid curve represents an inverse dependence on the AK gap.

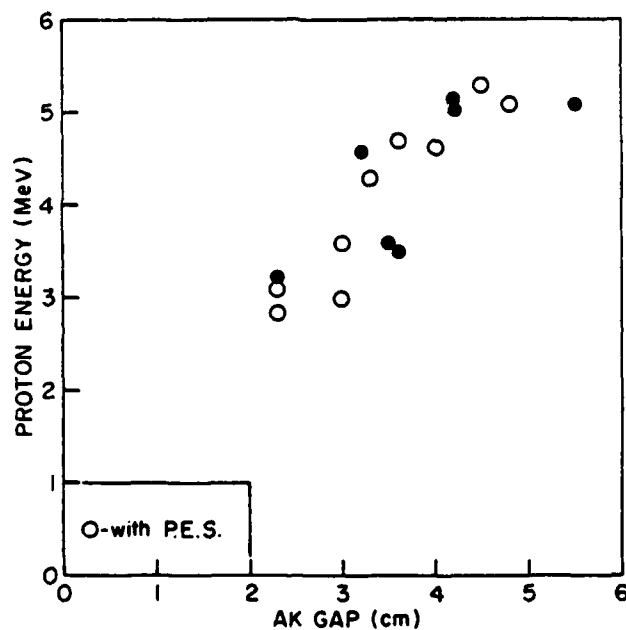
did not seem to affect the inverse dependence of the Rogowski current on the AK gap but did affect the shape of the Rogowski-current signal. With the PES system operating, the onset of the ion-current signal was delayed by ~ 50 ns, and the signal risetime was sharpened measurably. These observations are consistent with suppression of plasma formation in the diode by the PES system early in the voltage pulse.

The diode voltage was inferred from neutron TOF measurements using the ${}^7\text{Li}(p,n){}^7\text{Be}$ reaction. Neutron TOF traces for three different AK gaps are shown in Fig. 10a. As the AK gap is reduced, the neutron signal is delayed in time and is less intense. Measurable neutron traces were observed at small AK gaps by decreasing the neutron flight path. The neutron flight time was determined by measuring from the peak of the x-ray pulse to the leading edge of the neutron signal (50% of the peak) and correcting for the x-ray flight time. This measurement corresponds to the most energetic neutrons and consequently the most energetic protons from the diode. Proton energies extracted from such measurements using the ${}^7\text{Li}(p,n){}^7\text{Be}$ reaction kinematics¹⁵ are shown in Fig. 10b. These measurements have an uncertainty of ± 0.2 MeV due to the uncertainty in time between the x-ray and neutron signals. This measurement is difficult below 3 MeV because this reaction has a neutron-production threshold of 1.9 MeV. The dependence of the proton energy on AK gap is not sensitive to the use of the PES system (see Fig. 10b).

The proton intensity may be deduced from the measured neutron yield for comparison with the Rogowski-current measurements. Yields of 1 to 2×10^{11} neut/sr at 45° are measured for AK gaps of 2 to 5 cm. This yield is approximately constant as the AK gap is increased because the larger



(a) Neutron TOF signals measured for AK gaps of 5.5, 4.0 and 3.0 cm



(b) Dependence of the proton energy, determined from neutron TOF, on the AK gap. Shots with the PES system operating are plotted as open circles.

Figure 10

yield expected from increasing proton energy is compensated for by a decreasing proton current. The largest yield in these experiments is 2×10^{12} neutrons/pulse into 4π , which is only 20% of that obtained in the negative-polarity experiments.⁵ Power levels in this experiment were significantly less than in the negative-polarity experiments. The proton intensity is determined from the neutron yield by using thick-target yields⁵ at 45° for the ${}^7\text{Li}(p,n){}^7\text{Be}$ reaction and the proton energy determined from neutron TOF. Intensities range from 5×10^{15} protons for a 5-cm AK gap to 2×10^{16} protons for a 2-cm AK gap. These intensities correspond to proton currents of 8 kA and 30 kA respectively for a pulse duration of 100 ns. These currents are approximately one-half of the Rogowski-current measurements given in Fig. 9. Such a difference is consistent with average currents for neutron measurements compared with peak values from Rogowski-coil measurements.

To provide a representative diode impedance, the diode voltage, derived from a neutron TOF measurement, is divided by the peak diode current, as given by the shunt current (I_A). This impedance increases from about $10 \, \Omega$ at the smallest AK gap to $35 \, \Omega$ at the largest AK gap. The ion-generation efficiency is measured by the ratio, I_R/I_A . This ratio is 20% for a 2.5-MV, $10 \, \Omega$ diode with 2-cm AK gap. If the gap is increased to 5 cm, the ion efficiency is still 20% but the diode operates at 5 MV and $35 \, \Omega$. These results are similar to negative-polarity experiments for which the ion efficiency was 20% at 5 MV and $25 \, \Omega$.⁵ However, the negative-polarity experiments were carried out at a higher power level of ~ 1.2 TW.

In order to test the scaling of the ion-beam-generation efficiency, as described in Sec. II, the peak ion current from the Rogowski coil was

normalized to the electron current ($I_e = I_A - I_R$) and to the relativistic factor $(\gamma + 1)^{1/2}$ where $\gamma = [V_p / (M_e c^2) + 1]$ and V_p is the proton energy derived from neutron TOF. The dependence of these normalized quantities on the AK gap is shown in Fig. 11. Shots with the PES system are consistent with an inverse dependence on the AK gap as would be expected from the theory described in Sec. II. The non-PES shots fall to the right of the PES data in Fig. 11. Comparison of these data suggests that without the PES system, anode and cathode plasmas formed early in time result in a 1-cm greater closure of the AK gap than shots with the PES system. Gap closure of 1 cm without the PES is possible due to anode and cathode plasma formation either from the accelerator prepulse or during the rising portion of the diode voltage pulse. The data shown in Fig. 11 correspond to a value of $\frac{I_R}{I_e} (\gamma + 1)^{-1/2} = 0.09$ for a 2.5-cm AK gap using peak values for the various terms. This value is 2.5 times larger than that predicted for R/D scaling of the pinch-reflex diode. Such enhancement factors are consistent with previous experimental results on the other accelerators.¹⁶

V. Summary

In these first experiments performed in positive polarity on the Aurora accelerator the Marx generator and Blumlein operated satisfactorily at +90 KV Marx charge. A voltage dependent shortening of the pulse across the diode-insulator stack was observed and may be related to insulator flashover. This behavior is dependent on the diode impedance as determined by the AK gap in the pinch-reflex-diode geometry used in these experiments.

Plasma erosion switches were used in these experiments to eliminate

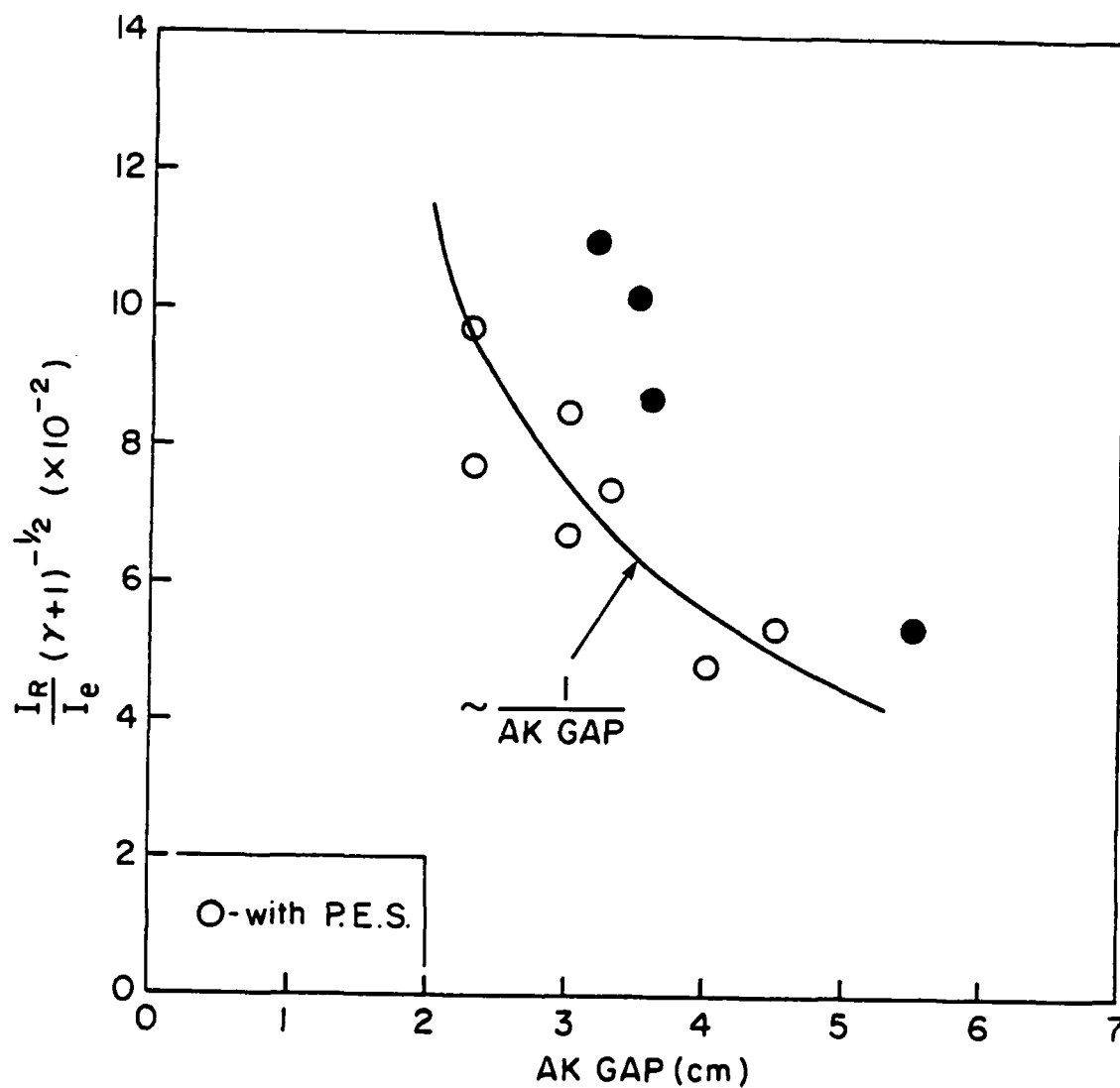


Fig. 11 — Dependence of the peak Rogowski-coil current, normalized according to Eq. 2, on the AK gap. Shots with the PES system operating are plotted as open circles. The solid curve represents an inverse dependence on the AK gap.

prepulse at the ion diode. These switches appeared to decrease AK gap closure by 1 cm, thereby allowing smaller AK gaps to be used without gap closure shorting the pulse prematurely.

Ion beams with peak net currents of 65 kA were measured for a 10- Ω , 2.5-MV diode configuration. The ion current appears to scale inversely with the AK gap. The ion efficiency is constant at 20% over the 10 to 35 Ω impedance range of this experiment. This effect may be due to the poor coupling of the low-impedance pinch-reflex diode to the 50- Ω transmission line of the Aurora accelerator which limited peak power levels to less than 1 TW. The ion efficiency of 20% is 2.5 times larger than that expected from pinch-reflex-diode theory and agrees with other pinch-reflex-diode experiments and numerical simulations.

Acknowledgments

The success of this experiment required the support and cooperation of many personnel. The conversion of the Aurora pulser to positive polarity was carried out under the direction of A. Stewart of the Harry Diamond Laboratories (HDL). The modifications to Aurora and the operation of the machine were ably handled by the Operations and Maintenance Staff of HDL under the supervision of A. Pourier or D. Lindsey. J. Shipman of Sachs-Freeman assisted in evaluating power-flow problems in positive polarity. Technical assistance with the experimental setup and data acquisition involved the support of the following personnel: S. Graybill, D. Whittaker, K. Kerris, C. Casaer, T. Cassidy and R. Bixby of HDL; R. Boller, J. Condon and T. Robinson of NRL; and D. Bacon of JAYCOR. Guidance and theoretical support were provided by G. Cooperstein of NRL, Shyke Goldstein of JAYCOR, and A. Drobot of SAI. C.W. Mendel, Jr., of Sandia National Laboratory provided plasma-erosion-switch hardware and technical support for their use. The encouragement and support of R. L. Gullickson of the Defense Nuclear Agency is also gratefully acknowledged. This work was supported by the Defense Nuclear Agency.

References

1. P.A. Miller; D.J. Johnson, T.P. Wright, and G.W. Kuswa, Comments Plasma Phys. 5, 95 (1979).
2. G. Cooperstein, Shyke A. Goldstein, D. Mosher, R.J. Barker, J.R. Boller, D.G. Colombant, A. Drobot, R.A. Meger, W.F. Oliphant, P.F. Ottinger, F.L. Sandel, S.J. Stephanakis, and F.C. Young, in Laser Interaction and Related Plasma Phenomena, edited by H. Schwarz, H. Hora, M. Lubin and B. Yaakobi (Plenum, New York, 1981) Vol. 5, p. 105.

3. S.J. Stephanakis, D. Mosher, G. Cooperstein, J.R. Boller, J. Golden, and Shyke A. Goldstein, Phys. Rev. Lett. 37, 1543 (1976).
4. S.J. Stephanakis, J.R. Boller, G. Cooperstein, Shyke A. Goldstein, D.D. Hinshelwood, D. Mosher, W.F. Oliphant, F.C. Young, R.D. Genuario, and J.E. Maenchen, Bull. Am. Phys. Soc., 24, 1031 (1979); and J. Maenchen, R. Genuario, R. Stringfield, J. Kishi, G. Cooperstein, D. Mosher, S. Stephanakis, F. Young, S. Goldstein and D. Hinshelwood, Bull. Am. Phys. Soc. 25, 945 (1980).
5. R.A. Meger, F.C. Young, A.T. Drobot, G. Cooperstein, Shyke A. Goldstein, D. Mosher, S.E. Graybill, G.A. Huttlin, K.G. Kerris and A.G. Stewart, J. Appl. Phys. 52, 6084 (1981).
6. B. Bernstein and I. Smith, IEEE Trans. Nucl. Sci. NS20, 294 (1973).
7. J.W. Poukey, Appl. Phys. Lett. 26, 145 (1975).
8. Shyke A. Goldstein and Roswell Lee, Phys. Rev. Lett. 35, 1079 (1975).
9. C.W. Mendel, Jr., D.M. Zagar, G.S. Mills, S. Humphries, Jr., and S.A. Goldstein, Rev. Sci. Instrum. 51, 1641 (1980).
10. C.W. Mendel, Jr., and S.A. Goldstein, J. Appl. Phys. 48, 1004 (1977).
11. F.C. Young, IEEE Trans. Nucl. Sci. NS-22, 718 (1975).
12. R.A. Meger, F.C. Young, A.T. Drobot, G. Cooperstein, Shyke A. Goldstein, D. Mosher, S.E. Graybill, G.A. Huttlin, K.G. Kerris, and A.G. Stewart, NRL Memorandum Report No. 4477, March, 1981 (unpublished).
13. I.D. Smith, Intl. Symposium on High Voltages in Vacuum, MIT, Cambridge, MA, Oct. 19-21, 1966 (unpublished).
14. A.T. Drobot, R.A. Meger, and Shyke A. Goldstein, Bull. Am. Phys. Soc., Ser. II, 25, 900 (1980).
15. H. Liskien and A. Paulsen, At. Nucl. Data Table 15, 57 (1975).
16. S.J. Stephanakis, private communication.

DISTRIBUTION LIST

Director
Defense Nuclear Agency
Washington, DC 20305

Attn: TISI Archieves 1 copy
TITL Tech. Library 3 copy
J. Z. FARBER (RAEV) 1 copy
R. L. Gullickson(RAEV) 1 copy

Air Force Office of Scientific Research
Physics Directorate
Bolling AFB, DC 20332

Attn: A. K. Hyder 1 copy
M. A. Strosio 1 copy

Air Force Weapons Laboratory, AFSC
Kirtland AFB, NM 87117

Attn: NTYP (W. L. Baker) 1 copy

BMO/EN
Norton AFB, CA

Attn: ENSN 1 copy
Commander
Harry Diamond Laboratory
2800 Powder Mill Rd.
Adelphi, MD 20733
(CNWDI-INNER ENVELOPE: ATTN: DELHD-RBH)

Attn: DELHD-NP 1 copy
DELHD-RCC - J. A. Rosando 1 copy
DRXDO-RBH - K. Kerris 1 copy
DRXDO-TI - Tech Lib. 1 copy

Defense Advanced Research Project Agency
1400 Wilson Blvd.
Arlington, VA 22209
Attn: J. Bayless 1 copy

Maxwell Laboratories, Inc.
9244 Balboa Avenue
San Diego, CA 92123

Attn: J. Pearlman 1 copy

Defense Technical Information Center
Cameron Station
5010 Duke Street
Alexandria, VA 22314 2 copies

Naval Research Laboratory
Addressee: Attn: Name/Code
Code 2628 - TIC Distribution 25 copies
Code 4040 - J. Boris 1 copy
Code 6682 - D. Nagel 1 copy
Code 4700 - S. L. Ossakow 26 copies
Code 4720 - J. Davis 1 copy
Code 4730 - S. Bodner 1 copy
Code 4740 - V. Granatstein 1 copy
Code 4760 - B. Robson 1 copy
Code 4704 - C. Kapetanakis 1 copy
Code 4770 - I.M. Vitkovitsky 10 copy
Code 4771 - F. C. Young 115 copies
Code 4773 - S. J. Stephanakis 1 copy
Code 4771 - D. Mosher 10 copies
Code 4773 - G. Cooperstein 10 copies
Code 4790 - D. Colombant 1 copy
Code 4790 - I. Haber 1 copy
Code 4790 - M. Lampe 1 copy
On-Site Contractors
Code 4770 - R. A. Barker 1 copy
Code 4770 - S. A. Goldstein 1 copy
Code 4770 - R. A. Meger 15 copies
Code 4770 - P. F. Ottinger 1 copy
Code 4770 - F. L. Sandel 1 copy
Code 4790 - A. Drobot 1 copy

DAT
ILM